Web Working Papers
by

The Italian Group of Environmental Statistics

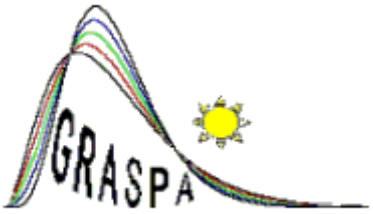

Gruppo di Ricerca per le Applicazione della Statistica
ai Problemi Ambientali

www.graspa.org

Space-time smoothed indicator kriging maps of risk for PM_{10} in Piemonte

Dana Draghicescu and Rosaria Ignaccolo

GRASPA Working paper n.25, April 2006

Space-time smoothed indicator kriging maps of risk for PM_{10} in Piemonte

Dana DRAGHICESCU
Hunter College of the City University of New York, USA

Rosaria IGNACCOLO[*]
University of Torino, Italy

February 20, 2006

Abstract

The Commission of the European Union, as well the United States Environmental Protection Agency (EPA) have set limit values for some pollutants in the ambient air, that have been showed to have adverse effects on human and environmental health. It is therefore important to identify areas where the risk to exceed these limit values is high. In this paper we focus on particulate matter with diameter less than 10 microns (PM_{10}). We exploit the space-time dependence of the underlying stochastic process to evaluate the probability to exceed the limit value fixed by law. We use records of daily measurements of PM_{10} at 22 locations in the North-Italian region Piemonte for the year 2004. We propose a two-step semiparametric procedure for the estimation of the probability to exceed the limit value set by law. Maps of these risks for the region of interest and a validation study illustrate the findings.

keywords: indicator kriging; maps of risk; PM_{10}; semiparametric models; smoothing; space-time dependence.

1 Introduction

The study of probability laws is fundamental in Statistics. When the data are not independent, modeling distribution functions become hard mathematical problems, with a wide area of applicability. Environmental science is one important field where many statistical contributions have been made, particularly in the past two decades. Environmental processes

[*]Corresponding author: R. Ignaccolo, Dipartimento di Statistica e Matematica Applicata, piazza Arbarello, 8, 10122 Torino (TO), Italy, email: ignaccolo@econ.unito.it. Work partially supported by Italian MIUR-Cofin 2004.

have been observed to have complex structures, generated by their temporal and spatial dependencies, that in many cases show significant departures from normality or stationary behavior. Examples include climatological processes (temperature, precipitation), and air pollution processes (ozone, particulate matter). Analysis of environmental data received much attention from both theoretical statisticians and mathematicians, as well as applied scientists in many fields. A theoretical motivation is given by the challenges connected to estimation and prediction for random fields, generated by the fundamental difference between one- and multidimensional processes. For example notions of past, future, memory have no direct analogy in space, and therefore space-time models need to be more flexible, as well as mathematically justifiable. Examples of practical motivations include understanding long-term variations in climate events, and spatial-temporal patterns of pollutants' elevated levels. This increasing scientific interest, intensified in recent years, is primarily generated by the adverse impacts of extreme weather phenomena on all spheres of life, and of the high levels of pollution on human and environmental health. While past studies have focused mainly on the behavior of trends (mean functions), comparatively little is known about the space-time variations of distribution functions for environmental processes. Moreover, it is often the case that many data are collected in the time domain, and considerable progress has been done during the past decades through understanding temporal variability. There exist many flexible statistical models suitable for complex time-dependent behavior, that need to be extended for the space-time case.

For instance, one way to generate one-dimensional dependent processes is via a time-varying transformation $G(t, Z_t)$ of a stationary process Z_t. By allowing the unknown transformation G to vary with time, the probability distribution function of the resulting process may also change, and therefore the process may not be stationary. Ghosh *et al.* (1997) studied the asymptotic properties of a nonparametric estimator of the marginal probability distribution function in this setting, where the underlying process Z_t was assumed to be Gaussian and having long memory. A similar estimator was analyzed in Draghicescu (2002, 2003), Draghicescu and Ghosh (2003) for the case when the underlying Gaussian process has short memory (under the general assumption that the correlations are summable). A data-driven procedure for optimal bandwidth selection for these kernel estimators was proposed in Ghosh and Draghicescu (2002) and discussed in detail in Draghicescu (2002, 2003). A new kernel distribution function estimator was recently discussed in Swanepoel and Van Graan (2005), where a data-based choise of bandwidth was also proposed. The method holds for independent, identically distributed (*iid*) data, however it can be extended for weakly dependent observations. Bosq (1998) provides a comprehensive overview of nonparametric methods for stochastic processes. However, there are many open problems regarding spatial modeling of distribution functions. One immediate, albeit naive approch is given by the so-called *indicator kriging* (Chilès and Delfiner 1999, p. 383), that is an adaptation of ordinary kriging (spatial interpolation). Recently Short et al. (2005) introduced a fully hierarchical approach for modeling distribution functions for bivariate spatial processes, using a Bayesian framework implemented via MCMC methods. To sum up, while temporal dependency is pretty well addressed in recent statistical literature, there is an increasing need for viable space-time

models.
As regards air pollution, the Commission of the European Union as well as the U.S. EPA have set limit values for some pollutants in the ambient air, that were proved to have a negative impact on human and environmental health. In particular, recent studies linked traffic-related pollutants to increased risks of morbidity and mortality due to respiratory and cardiovascular illness (see for example Samet et al. 2000 and the references therein). It is therefore important to identify areas where the risk to exceed these limit values is high.
In this paper we focus on particulate matter with diameter less than 10 microns (PM_{10}). Exploratory analyses and basic statistical models for this pollutant were employed in McKendry (2000), Kingham et al. (2000), Ignaccolo and Nicolis (2005), Rajsic et al. (2004), among others. A review of recent studies on particulate matter is given in Schimek (2003), where a semiparametric model including weather information is used to link particulate matter to hospital admissions in a regional study, controlling for potential spatial dependencies. In contrast to these studies, where PM_{10} is modeled directly, we focus on the probability of exceeding the limit value imposed by law. We use a two-stage semiparametric procedure to estimate the space-time risk of exceeding a given threshold. The paper is organized as follows. The data set that motivated this study is described in Section 2. Section 3 is devoted to statistical methodology, followed by applications and a validation study in Sections 4, 5 respectively. Concluding remarks are given is Section 6.

2 A motivating data set

We analyze daily PM_{10} concentrations (in $\mu g/m^3$) during 2004 at 22 sites in the North-Italian region Piemonte. The data were collected through the information system *AriaWeb Regione Piemonte.* A detailed description of this monitoring network can be found in Ignaccolo and Nicolis (2005). The 22 records used in this study were selected from Low Volume Gravimetric (LVG) monitors, such that the amount of missing data did not exceed 10%. The missing values were imputed by using kernel regression smoothing with adaptive plug-in bandwidth (Gasser et al. 1991). The maximum number of days with threshold exceeding 50 $\mu g/m^3$ is set by law to 35. Thus 50 $\mu g/m^3$ is the threshold for the sample 0.904 quantile during one year. Detailed explanations of the european norms for air pollution are given in van Aalst et al. (1998). Figure 1 shows the locations of these 22 sites, together with the respective 0.904 quantiles. It can be observed that the sites near the Alps have lower PM_{10} values, whereas higher pollution levels are detected in the valleys, closer to urban areas. Figure 2 displays boxplots of the autocorrelation functions for these 22 time series, indicating short-range temporal dependence. The same data set is used in Bande, Ignaccolo and Nicolis (2006), where additional meteorological and geographical information is included in a model for the space-time PM_{10} trend (mean function). As regards modeling the probability of exceeding the cutoff PM_{10} value set by law, the preliminary study Draghicescu and Ignaccolo (2005) proposes a semiparametric modeling technique for maps of risk in the same region, using data from 17 monitors for the year 2003. This method will be briefly described in Section 4, applied to the 2004 data set, and used for comparisons in Sections 4 and 5.

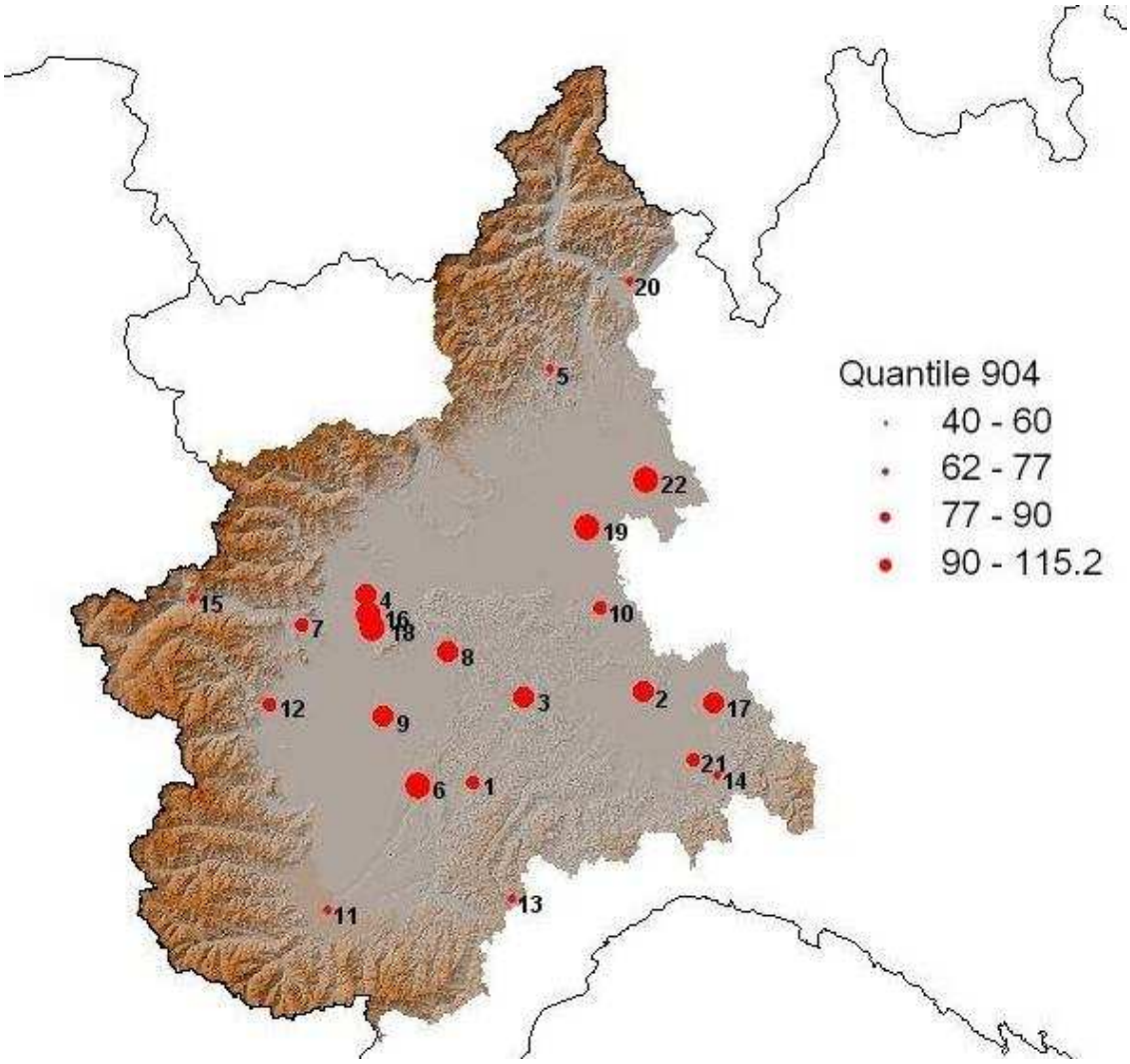

Figure 1: Locations of 22 air pollution monitoring stations in Piemonte; superimposed 2004 annual 0.904 quantiles of daily PM_{10} ($\mu g/m^3$).

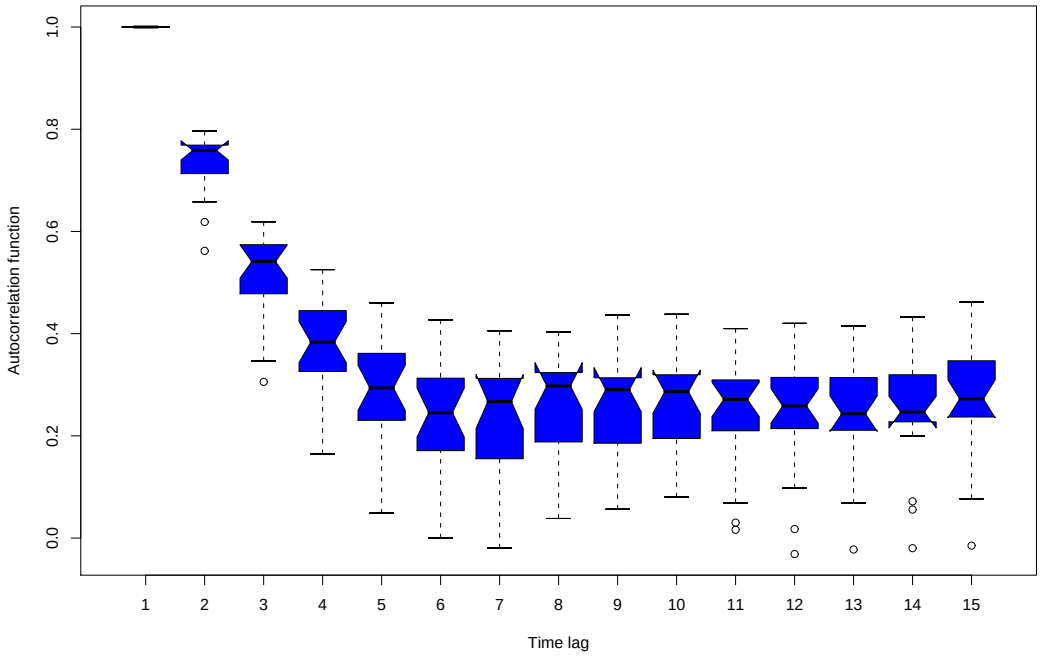

Figure 2: Boxplots (over the 22 locations) of the empirical autocorrelation functions for the time series of daily PM_{10} at the 22 locations, year 2004.

3 A statistical model for space-time risks

3.1 Definitions, notations and assumptions

Assume that at each location $s \in D$ (for some domain $D \in \mathbf{R}^2$) we observe a temporal process of the form $X_s(t) = G_s(t, Z_s(t))$, where G_s is an unknown transformation, Z_s is a standardized stationary Gaussian process with $\gamma_s(l) := cov(Z_s(t), Z_s(t+l))$, such that $\sum_{l=-\infty}^{\infty} |\gamma_s(l)| < \infty$. Note that this is a very general class of stochastic processes, including nonstationary and nongaussian situations, and thus suitable to model complex environmental data sets. Also, no parametric assumptions are made on the temporal covariance structure of the process.

For fixed $x_0 \in \mathbf{R}$, define the risk process $R_{x_0}(t, s) = P(X_s(t) \geq x_0)$. By using the axioms of probability, it is immediate to see that $R_{x_0}(t, s)$ takes values in $[0, 1]$ and is non-increasing in x_0. The problem of interest is to predict $R_{x_0}(t, s^*)$ at a location $s^* \in D$ where there are no observations, for any time t, based on observations of the process $X_s(t)$ at n time points $t_1, \ldots, t_n$ and at m spatial locations $s_1, \ldots, s_m$. Typically m is much smaller than n. Furthermore, for fixed t, the risk process is assumed to be isotropic in space, that is, all spatial covariances depend only on the Euclidean distance between the respective locations ($cov(R(t, s_i), R(t, s_j)) = C_t(||s_i - s_j||)$ for all $s_i, s_j \in D$).

The method we propose consists of 2 steps. We start by modeling the temporal risks for any location where the process is observed. Let $X_s(t_1), \ldots, X_s(t_n)$ be the daily PM_{10} observed concentrations, assumed to be realizations of a process $X_s(t) = G_s(t, Z_s(t))$ and x_0 the PM_{10} limit concentration set by law. We stress again that the true risk may change with time and space. Therefore the empirical risk estimator $R_{n,m}(x_0) := \frac{1}{nm}\sum_{i=1}^{n}\sum_{j=1}^{m} 1_{\{X_{s_j}(t_i)\geq x_0\}}$ (analoguous to the empirical distribution function) is too rough, and cannot capture such changes, making it necessary to consider different weights, that should depend on the local behavior of the process. As the problem of interest is not to assess the mean function of the process, but the probability to exceed the given threshold x_0, we need to focus on the indicator process $1_{\{X_s(t)\geq x_0\}}$. We assume further that the changes of this indicator process with time are smooth for all $s \in D$, namely that $1_{\{X_s(t_i)\geq x_0\}} - R_{x_0}(t_i, s) = \sum_{k=1}^{\infty} c_{k,s,x_0}(t_i)H_k(Z_s(t_i))$, where $t_i = \frac{i}{n}$ are rescaled time points, H_k denotes the Hermite polynomial of degree k, and the coefficients c_{k,s,x_0} are twice continuously differentiable with respect to t, and continuous with respect to s and x_0. For examples of time-varying transformations of Gaussian processes and detailed explanations of assumptions similar to the ones above, we refer to Draghicescu (2002, 2003). In the second step we use classic spatial interpolation to estimate the desired risk at any location in the region of interest.

3.2 Estimation of temporal risks

In the initial step we model the temporal risks nonparametrically, by using the Nadaraya-Watson kernel estimator

$$\hat{R}_{x_0}(t, s) = \frac{\sum_{i=1}^{n} K\big(\frac{t_i - t}{b_t}\big) 1_{\{X_s(t_i)\geq x_0\}}}{\sum_{i=1}^{n} K\big(\frac{t_i - t}{b_t}\big)}, \tag{1}$$

where K is a kernel function. For details on kernel smoothing we refer to Wand and Jones (1995). Note that the temporal bandwidth b_t should not depend on the threshold x_0, in order for the resulting estimator to be a proper risk function. In what follows, to keep notations simple, we write b instead of b_t.

Theorem 3.1. *In the above notations, if* $\frac{\partial^2}{\partial t^2}\Big[R_{x_0}(t, s)\Big]$ *exist a.e. in* $[0, 1]$ *and if* $\frac{\partial^2}{\partial t^2}\Big[Var\big(1_{\{X_s(t)\geq x_0\}}\big)\Big] < \infty$, *as* $n \to \infty$, $b \to 0$ *and* $nb \to \infty$, *for all* $s \in D$ *and fixed* $x_0 \in \mathbf{R}$, *for the estimator (1) we have*

(a) Consistency:

$$MSE\Big(\hat{R}_{x_0}(t, s)\Big) = O\Big(max\big(b^4, \frac{1}{nb}\big)\Big). \tag{2}$$

(b) Asymptotic normality:

$$\frac{\hat{R}_{x_0}(t,s) - E\hat{R}_{x_0}(t,s)}{\sqrt{Var\Big(\hat{R}_{x_0}(t,s)\Big)}} \longrightarrow_d N(0,1). \tag{3}$$

Sketch of the proof.
By using Taylor expansions, it is immediate to show that $Bias\Big(\hat{R}_{x_0}(t,s)\Big) := E\hat{R}_{x_0}(t,s) - R_{x_0}(t,s) = B(t,s,x_0)b^2 + o(b^2)$, where $B(t,s,x_0) = \frac{1}{2}\frac{\partial^2}{\partial t^2}\Big[R_{x_0}(t,s)\Big]\int u^2K(u)du$.
Also, $Var\Big(\hat{R}_{x_0}(t,s)\Big) = \frac{1}{nb}V(t,s,x_0) + o\big(\frac{1}{nb}\big)$, where $V(t,s,x_0) < M$ for some nonnegative constant M. Consistency then follows from Chebyshev's inequality. The Central Limit Theorem is an immediate application of results in Breuer and Major (1983).

Remark 3.1. *Estimator (1) has the same rate of convergence as in the iid case.*

Remark 3.2. *An optimal bandwidth can be obtained by minimizing the mean squared error of the estimator (1). Note that, as in the iid case, $b_{opt} \sim Cn^{-\frac{1}{5}}$. In practice, an optimal bandwidth (local or global) can be obtained by using plug-in estimators (approximations) of the bias and variance (see for example Ghosh and Draghicescu 2002, Draghicescu 2002, 2003). While local time-dependent bandwidths have the advantage of dealing with edge effects (at the ends of the time interval), it is often the case that global (integrated over time) bandwidths considerably decrease computational time, without significant change in the resulting estimators.*

3.3 Spatial interpolation

In the second step we use use spatial interpolation with Matèrn covariance function to predict the risk field field at a location $s^* \in D$ where there are no observations. The threshold x_0 is fixed. To keep notations simple and without confusion we will omit it in expression (4) below. Extensive exploratory analyses performed on this data set did not detect major violations of spatial isotropy (that is, the spatial correlations only depend on distance and not on direction). Therefore we use this assumption and model the spatial covariance function of the estimated temporal risks by

$$C_t(||s_i - s_j||) := Cov\big(\hat{R}(t,s_i), \hat{R}(t,s_j)\big) = \frac{\sigma_t}{2^{\nu_t - 1}\Gamma(\nu_t)}\Big(\frac{2\sqrt{\nu_t}||s_i - s_j||}{\rho_t}\Big)^{\nu_t}\mathcal{K}_{\nu_t}\Big(\frac{2\sqrt{\nu_t}||s_i - s_j||}{\rho_t}\Big) \tag{4}$$

for any fixed day t. This is the well known Matèrn class (see Stein 1999, Chapter 2 for details). $\Gamma(\cdot)$ is the usual gamma function and $\mathcal{K}_{\nu_t}(\cdot)$ is the modified Bessel function of the third kind of order ν_t. The parameter $\nu_t > 0$ characterizes the smoothness of the process, σ_t denotes the variance of the transformed random field, and ρ_t measures how quickly the correlations of this field decay with distance. These parameters are estimated by maximum likelihood. Spatial interpolation is then used to produce the desired estimates $\hat{R}_{x_0}(t,s^*)$ for

any unknown location $s^* \in D$ and any day in the period of interest. For details on spatial interpolation we refer to Stein 1999, Chapter 1.
As mentioned in the Introduction, another way of getting spatial maps of risk is given by indicator kriging. This approach considers estimators/predictors as linear combinations of the observed indicators. As with ordinary kriging (spatial interpolation), the aforementioned weights are uniquely determined from a given (known) space-time covariance function of the respective process, that is typically modeled parametrically (for example by using the flexible Matèrn class given by (4)).

Remark 3.3. *Linear interpolation does not guarantee that the resulting risk estimator/predictor takes values in the interval* $[0,1]$. *A* $1:1$ *transformation* $g:[0,1] \to \mathbf{R}$ *(such as* $g(x) = log\left(\frac{x}{1-x}\right)$ *for example) can be used first, then perform interpolation on the transformed field, and finally invert to obtain the desired risks. However, this technical detail did not provide improved maps of risk for the present study.*

4 Maps of risk for PM_{10} in Piemonte

We applied the methodology described in the previous section to the Piemonte PM_{10} data. We estimated the risks of exceeding 50 $\mu g/m^3$ for each day. In order get a better understanding of the underlying stochastic process, as well as to assess the performance of our mapping procedures, we used the following three methods. They are all semiparametric and carried out in two stages, the second one being the same in all three cases (ordinary kriging with Matèrn covariance function). As the number of spatial locations where the process is observed is relatively small (22), spatial interpolation provides the best (minimum variance) predictors for any location in the region. The first method that we applied is the indicator kriging, i.e. spatial interpolation of the empirical risk process. It will be referred to as **IND.** The next approaches require a preliminary smoothing step in the temporal domain. Thus, the second method, referred to as **EDF**, is the two-step procedure introduced in Draghicescu and Ignaccolo (2005). For every day t_i, a weight is assigned to the observed risk 0 or 1, corresponding to the order of the quantile of the PM_{10} observation for that day (i.e. the empirical distribution function EDF). For example, if the observed value is 80, and 75% of the data in the year are less than 80, the respective weight will be 0.75, i.e. EDF(80). Then the risk is estimated by a weighted average of the observed risks on a time window centered at day t_i. In the following applications and validation study the window width was fixed and equal to 7 days. The third method, called **KER** is based on kernel smoothing, as described in detail in Section 3.
Figure 3 displays these risks on February 18, 2004 (left) and February 19, 2004 (right) based on the aforementioned methods. On February 18 the maximum value of PM_{10} for 2004 was observed at all sites, with a large decrease the following day. In this case IND does not seem to work so well, the maps look too rough and there is an abrupt change from a day to the next. The unshaded region on the February 19 map is due to negative values of the predicted risks, that, for the applied goal of this study, can be viewed as zeros. EDF yields

maps with high values on almost all the region, while KER shows higher values around the Torino area. As observations outside Piemonte were not available, the estimated risks near the boundaries tend to have larger errors.
While these methods provide maps of point estimates, and could give a good understanding of the process (by using animation techniques for example), it is often the case that transformations of point estimates are also of interest. For instance seasonal averages are very iformative summaries for both scientists and policy makers. Figure 4 shows estimated risks to exceed $50\mu g/m^3$ averaged over summer (left) and winter (right), again obtained through the three methods. Summer is considered the period between April 1st and September 30th. From a geographical prospective these methods yield maps that are not very different. However, from a statistical point of view, EDF or KER have the advantage of making use of all the information in the data. As expected, in both seasons the highest risks are around the Torino area, with larger values during the winter.

5 Validation

The following validation study was carried out in order to assess the performance of these methods. We used the leave-one-out principle and estimated the daily risks to exceed 50 $\mu g/m^3$ at each site, based on observations at the remaining 21 sites for each day. Each row in Table 1 corresponds to a monitoring location, labeled as in Figure 1, and displays the root mean squared prediction errors obtained by leaving out that site, computed as the square root of the averages (over the 366 days of the year 2004) of squared risk differences (observed - predicted).
While all the errors are quite small, IND seems to do better than the other two methods in most cases, however, this behavior may be explained by the fact that only values of 0 and 1 are interpolated. EDF and KER yielded comparable results, the respective errors being smaller for KER at 16 of the sites.

6 Conclusion

The methodology proposed in this paper provides a good descriptive and modeling tool for space-time data with large temporal and relatively small spatial coverages. It is computationaly fast, statistically accurate, and flexible enough to be suitable for processes with complex space-time dependencies in many applied fields, such as environmental science and management, athmospheric sciences, ecology, epidemiology, etc.. Not only the KER method has rigorous mathematical justification, it also produces smooth, nicer looking pictures.

Aknowledgements. The authors kindly thank Giorgio Arduino, who provided useful information and access to data, and Stefano Bande, who helped with the geocoding for the air pollution maps. Research for this project and collaboration between the authors began

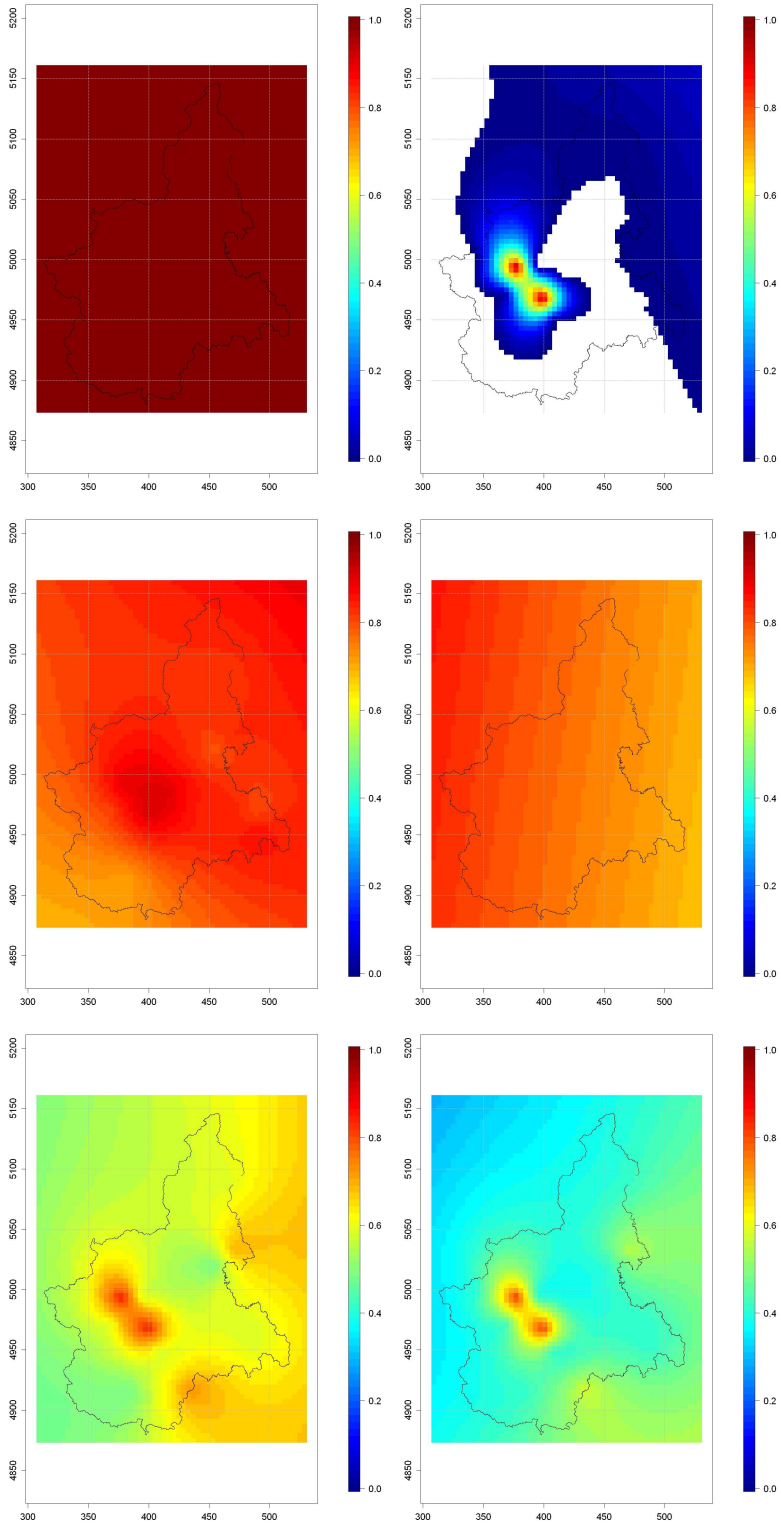

Figure 3: Estimated risks to exceed $50\mu g/m^3$ on February 18, 2004 (left) and February 19, 2004 (right); IND (top), EDF (middle), KER (bottom).

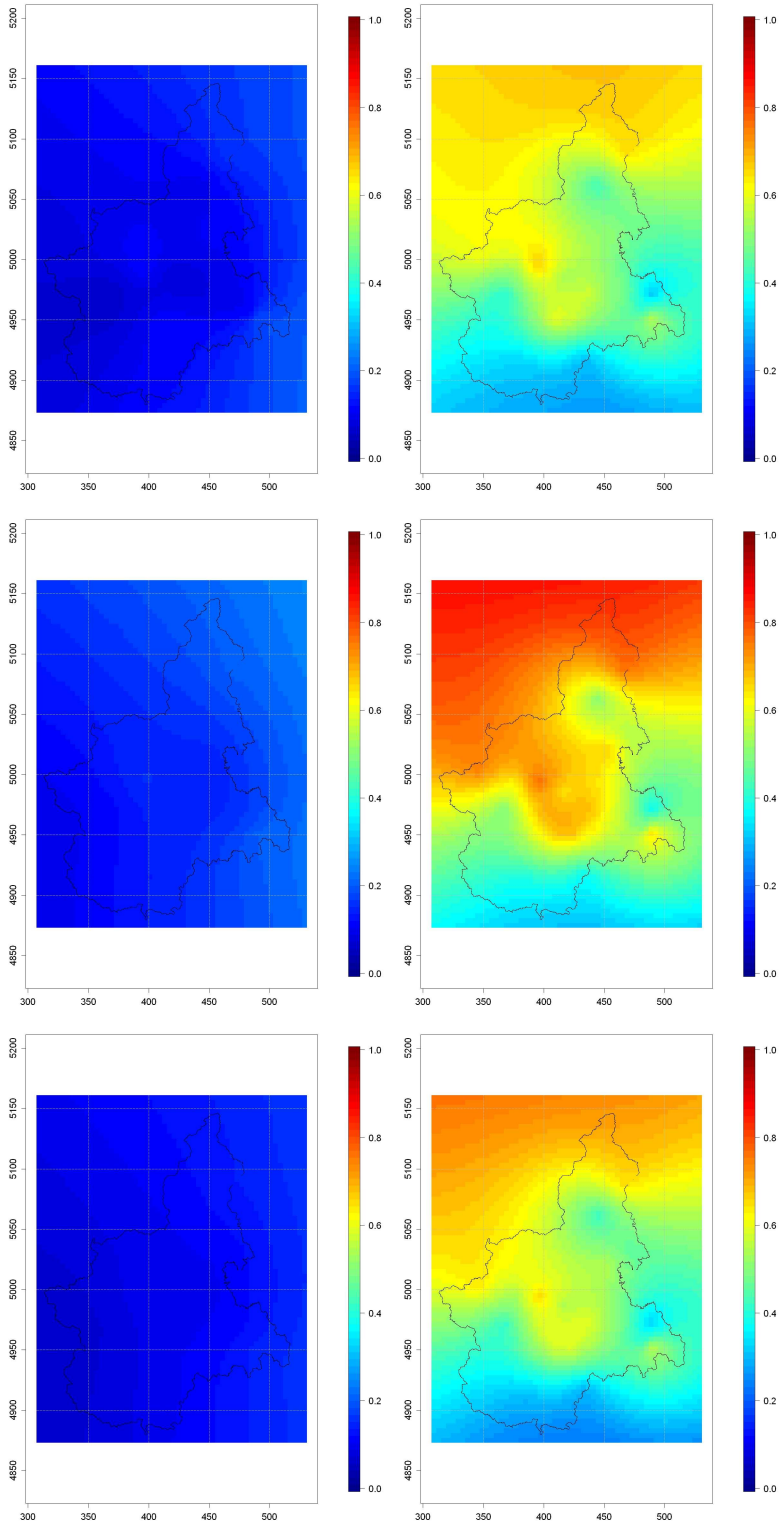

Figure 4: Estimated risks to exceed $50\mu g/m^3$ averaged over summer (left) and winter (right); IND (top), EDF (middle), KER (bottom).

	Site	IND	EDF	KER
1	AL - Nuova Orti	0.189	0.312	0.284
2	Alba	0.329	0.358	0.359
3	AT - Scuola D'Acquisto	0.269	0.313	0.297
4	Borgaro	0.285	0.361	0.332
5	Borgosesia	0.477	0.514	0.449
6	Bra	0.362	0.375	0.378
7	Buttigliera Alta	0.353	0.393	0.367
8	Buttigliera d'Asti	0.329	0.393	0.349
9	Carmagnola	0.326	0.356	0.338
10	Casale Monferrato - Via De Negri	0.337	0.367	0.334
11	CN - Piazza II Reggimento Alpini	0.365	0.405	0.377
12	NO - Viale Roma	0.384	0.407	0.373
13	Novi Ligure	0.459	0.497	0.428
14	Pinerolo	0.396	0.447	0.390
15	Saliceto	0.411	0.425	0.385
16	Serravalle Scrivia	0.735	0.696	0.716
17	Susa	0.398	0.406	0.395
18	TO - I.T.I.S. GRASSI	0.388	0.393	0.405
19	TO - Via Consolata	0.325	0.344	0.352
20	Tortona	0.403	0.428	0.378
21	VC - Corso Gastaldi	0.343	0.373	0.363
22	Verbania	0.503	0.439	0.451

Table 1: Root mean squared errors: $RMSE = \sqrt{\frac{1}{366}\sum_{i=1}^{366}(O_i - P_i)^2}$, where O_i is the observed risk and P_i is the predicted risk at day i.

in Chicago in August 2004 and continued in New York, Messina, Oslo, Paris, Torino. The authors are very grateful for the many encouraging comments from friends and colleagues, that made working on this study a very enjoyable experience.

References

R. van Aalst, L. Edwards, T. Pulles, E. De Saeger, M. Tombrou, D. Tonnesen (1998). Guidance report on preliminary assessment under EC air quality directives. Technical report no. 11, European Environment Agency.

S. Bande, R. Ignaccolo and O. Nicolis (2006). Spatio-temporal modelling for PM_{10} in Piemonte. (*submitted*, SIS 2006)

D. Bosq (1998). Nonparametric statistics for stochastic processes. Estimation and prediction (second edition). Springer.

P. Breuer and P. Major (1983). Central limit theorems for non-linear functionals of Gaussian fields. J. Multiv. Analysis, **13**:425–441.

J.-P. Chilès and P. Delfiner (1999). Geostatistics: modeling spatial uncertainty. John Wiley & Sons.

D. Draghicescu and R. Ignaccolo (2005). Spatio-temporal maps of risk for PM_{10} in Piemonte. Contributed papers for the Italian Statistical Society Meeting "Statistics and Environment", CLEUP, 275–278.

D. Draghicescu (2003). Optimal bandwidth selection for kernel estimatorsof time-varying quantiles. Technical report no. 2, CISES, The University of Chicago.

http://galton.uchicago.edu/∼cises/research/cises-tr2.pdf

D. Draghicescu and S. Ghosh (2003). Smooth nonparametric quantiles. Proceedings, MENP-2, Bucharest, Romania. Geometry Balkan Press, 45–52.

D. Draghicescu (2002). Nonparametric quantile estimation for dependent data. Thesis no. 2592, Federal Institute of Technology Lausanne (EPFL), Switzerland.

T. Gasser, A. Kneip, W. Koehler (1991). A flexible and fast method for automatic smoothing. *JASA*, **86**:643–652.

S. Ghosh, J. Beran and J. Innes (1997). Nonparametric conditional quantile estimation in the presence of long-memory. *Student*, **2**:109–117.

S. Ghosh and D. Draghicescu (2002). An algorithm for optimal bandwidth selection for smooth nonparametric quantile estimation. Statistical Data Analysis Based on the L1-Norm and Related Methods. Birkhäuser, 161–168.

R. Ignaccolo and O. Nicolis (2005). Analisi Statistica Preliminare della Dinamica Spazio-Temporale dei PM_{10} in Piemonte. *Technical Report DIGI Department* MS Series, **8**.

http://www.unibg.it/dati/bacheca/434/16817.pdf

I. G. McKendry (2000). PM_{10} levels in the lower Fraser Valley, British Columbia, Canada: An overview of spatiotemporal variations and meteorological controls. *Journal of the Air & Waste Management Association*, **50**:443–452.

E. Nadaraya (1964). On estimating regression. Theory Probab. Appl., **9**:141–142.

S. Rajsic, M. Tasic, V. Novakovic and M. Tomasevic (2004). First Assessment of the PM10 and PM2.5 Particulate Level in the Ambient Air of Belgrade City. *Environmental Science and Pollution Research*, **3**:158–164.

J. M. Samet, F. Dominici, F. C. Curriero, I. Coursac and S. L. Zeger (2000). Fine Particulate Air Pollution and Mortality in 20 U.S. Cities, 1987–1994. *The New England Journal of Medicine*, **343**:1742–1749.

M. G. Schimek (2003). Controlling spatial dependence between a PM study region and its background in a semiparametric model. *Proceedings, The ISI International Conference on Environmental Statistics and Health.* Universidade de Santiago de Compostela publicacions, 111–119.

M. Short, B. P. Carlin and A. Gelfand (2005). Bivariate spatial process modeling for constructing indicator or intensity weighted spatial CDFs. *JABES*, **10**(3):259–275.

M. L. Stein (1999). Interpolation for spatial data: some theory of kriging. Springer, New York.

J. W. H. Swanepoel and F. C. Van Graan (2005). A new kernel distribution function estimator based on a non-parametric transformation of the data. *Scandinavian Journal of Statistics*, **32**:551–562.

M. P. Wand and M. C. Jones (1995). Kernel smoothing. Chapman & Hall.

G. Watson (1964). Smooth regression analysis. Sankhya, Series A, **26**:359–372.